Dyadic Tensor-Based Interpolation of Tensor Orientation: Application to Cardiac DT-MRI*

Jin Kyu Gahm[1,2] and Daniel B. Ennis[2]

[1] Department of Computer Science, UCLA, CA 90095, USA
[2] Department of Radiological Sciences, UCLA, CA 90095, USA
gahmj@ucla.edu

Abstract. *Objective*: To develop an accurate and mathematically unambiguous method for interpolation of tensor orientation, specifically for the interpolation of cardiac microstructural orientation. *Methods*: A dyadic tensor-based (DY) orientation interpolation method, which sidesteps the eigenvector sign ambiguity problem by interpolating between the dyadic tensors of eigenvectors, is proposed and evaluated. The quaternion-based (QT) orientation interpolation method, which interpolates along the minimum rotation path between tensor orientations, is also revised and evaluated. DY and QT are compared to conventional tensor-based interpolation methods using both synthetic and cardiac DT-MRI data. *Results*: All methods (except QT) perform similarly well for recovery of the primary eigenvector. DY has significantly less bias than all other methods for recovery of the secondary and tertiary eigenvector, which is especially important for interpolating myolaminar sheet orientation. *Conclusion*: DY is a fast, commutative, and mathematically unambiguous tensor orientation interpolation method that accurately interpolates cardiac microstructural orientation.

1 Introduction

Diffusion tensor magnetic resonance imaging (DT-MRI) [1] characterizes soft tissue microstructural organization by measuring, for example, tissue anisotropy and myofiber and myolaminae orientations. DT-MRI methods estimate the self-diffusion tensor of water in each image voxel. The second-order symmetric positive definite diffusion tensor ($\mathbf{D}$) can be decomposed into eigenvalues (λ_i, shape) and eigenvectors ($\mathbf{e}_i$, orientation). Tensor shape can also be intuitively and saliently represented by tensor invariants such as tensor trace (J_1), fractional anisotropy (FA, J_2) and tensor mode (J_3) [2–5].

The three eigenvectors correspond to the myofiber long-axis ($\mathbf{e}_1$), the cross-fiber direction within the myolaminar sheet ($\mathbf{e}_2$) and the sheet-normal direction ($\mathbf{e}_3$) in cardiac applications [6]. To build computational models of cardiac mechanics and electrophysiology (EP), both myofiber and myolaminae orientation

* This work was supported, in part, by grant support from the NIH (P01 HL78931) and the Department of Radiological Sciences at UCLA.

O. Camara et al. (Eds.): STACOM 2013, LNCS 8330, pp. 135–142, 2014.
© Springer-Verlag Berlin Heidelberg 2014

information is required at millions of closely spaced nodes. DT-MRI measurements, however, are on a lattice and typically number $<$ 1e6 for *ex vivo* studies $<$ 1e4 for *in vivo* studies [7], so interpolation of tensor orientation is needed. The orientation (SO(3)) interpolation problem has been widely studied in the computer graphics literature, but the tensor orientation interpolation problem in DT-MRI is more challenging because eigenvectors have an arbitrary sign (physiologically and mathematically) so tensor orientation cannot be uniquely described.

Most of the conventional approaches have been tensor-based and amongst the simplest is the Euclidean (EU) method, but it suffers from the tensor shape swelling effect [8, 9]. The affine-invariant Riemannian (AI) and log-Euclidean (LE) tensor interpolation methods [8, 9] were proposed to solve the tensor shape (tensor swelling) problem, but they underestimate other tensor invariants including tensor trace and FA [5, 10]. The geodesic-loxodrome (GL) method [4] guarantees monotonic interpolation of orthogonal tensor invariants [2], but is computationally expensive. The linear invariant (LI) method [5] linearly interpolates tensor invariants (shape) at significantly reduced computational cost, but no new method for tensor orientation interpolation was presented. The tensor-based methods mostly focus on tensor shape interpolation, and no distinct advantage of the methods in tensor orientation has been reported [5]. Recently a separate tensor interpolation method [10] was proposed that interpolates Euler angles or quaternions along the minimum rotation path between tensor orientations, but it was not quantitatively validated using cardiac DT-MRI data.

We propose a new dyadic-tensor based (DY) tensor orientation interpolation method that sidesteps the eigenvector sign ambiguity problem by interpolating between the dyadic tensors of eigenvectors with subsequent reduction to rank-1 dyadics and orthogonal matrices. We also revise and simplify the quaternion-based (QT) method [10], and evaluate it using cardiac DT-MRI data. The QT and DY tensor-based methods are compared to the tensor-based interpolation methods including EU, AI, LE and GL for accurate recovery of cardiac microstructural orientation using four experimentally measured DT-MRI datasets from rabbit and pig hearts.

2 Theory

Quaternion-Based Interpolation. One approach to resolve the eigenvector sign ambiguity problem is to directly tackle it by choosing the minimum rotation path between tensor orientations. Tensor orientation is commonly represented by a rotation matrix $\mathbf{R} = [\mathbf{e}_i]$ consisting of three eigenvectors, sorted in descending order of their corresponding eigenvalues, but can also be represented by a unit quaternion $\mathbf{q} = a + bi + cj + dk = [a, b, c, d]$ where $a^2 + b^2 + c^2 + d^2 = 1$. Tensor orientation has four different descriptions intuitively represented by rotation matrices $\mathbf{RP}$ where $\mathbf{P} = \mathrm{diag}(p_j)$ such that $p_j = \pm 1$ and $p_1 p_2 p_3 = 1$, which can be converted into unit quaternions $\mathbf{q}_k$:

$$\mathbf{q}_k = [a, b, c, d], [b, -a, d, -c], [c, -d, -a, b], [d, c, -b, -a] \; . \tag{1}$$

Then the minimum rotation path between two tensor orientations $\mathbf{R_A}$ and $\mathbf{R_B}$ can be determined by the maximum magnitude of inner products between fixed $\mathbf{q_A}$ and four different $\mathbf{q_B}$ (or between fixed $\mathbf{q_B}$ and four different $\mathbf{q_A}$). If the maximum value has a negative sign, the corresponding quaternion $\mathbf{q_B}$ (or $\mathbf{q_A}$) should be negated. Once the unit quaternions are uniquely determined, normalized linear interpolation (nlerp) is used:

$$\mathbf{q_C} = \left((1-t)\mathbf{q_A} + t\mathbf{q_B}\right) / \|(1-t)\mathbf{q_A} + t\mathbf{q_B}\| \ , \tag{2}$$

which is computationally less expensive than spherical linear interpolation (slerp) [11]. The interpolated quaternion $\mathbf{q_C}$ is easily converted to a rotation matrix $\mathbf{R_C}$.

Dyadic Tensor-Based Interpolation. Our approach is to sidestep the sign ambiguity problem by using dyadic tensors [12]. Dyadic tensors of eigenvectors $\mathbf{e}_i$ are defined by $\mathbf{E}_i = \mathbf{e}_i \otimes \mathbf{e}_i = \mathbf{e}_i\mathbf{e}_i^T$. Note, $\mathbf{e}_i \otimes \mathbf{e}_i = -\mathbf{e}_i \otimes -\mathbf{e}_i$. Dyadic tensors are rank-1 with only one non-zero eigenvalue whose value is 1 and the corresponding eigenvector is exactly $\mathbf{e}_i$ or $-\mathbf{e}_i$. Interpolation between $\mathbf{R_A} = [\mathbf{e_A}_i]$ and $\mathbf{R_B} = [\mathbf{e_B}_i]$ starts with linear interpolation between their dyadic tensors:

$$\mathbf{F}_i = (1-t)\mathbf{E_A}_i + t\mathbf{E_B}_i \ . \tag{3}$$

Since $\mathbf{F}_i$ are not generally rank-1, the nearest rank-1 dyadic tensor $(\mathbf{x} \otimes \mathbf{x})$ can be obtained by minimizing:

$$\begin{aligned} J(\mathbf{x}) &= \|\mathbf{F}_i - \mathbf{x} \otimes \mathbf{x}\|_F^2 = \mathrm{tr}\left\{(\mathbf{F}_i - \mathbf{x}\mathbf{x}^T)^T(\mathbf{F}_i - \mathbf{x}\mathbf{x}^T)\right\} \\ &= \mathrm{tr}\left\{\mathbf{F}_i^2 - 2\mathbf{F}_i\mathbf{x}\mathbf{x}^T + (\mathbf{x}\mathbf{x}^T)^2\right\} = \|\mathbf{F}_i\|_F^2 - 2\mathrm{tr}(\mathbf{x}^T\mathbf{F}_i\mathbf{x}) + \|\mathbf{x}\|^4 \ , \end{aligned} \tag{4}$$

where $\|\cdot\|_F$ denotes the Frobenius norm, and the derivative is:

$$J'(\mathbf{x}) = -4\mathbf{F}_i\mathbf{x} + 4\|\mathbf{x}\|^2\mathbf{x} \ . \tag{5}$$

By setting the derivative equal to zero, the eigenvalue equation $\mathbf{F}_i\mathbf{x} = \|\mathbf{x}\|^2\mathbf{x}$ is obtained. Therefore, the eigenvector $\mathbf{m}_i$ corresponding to the largest eigenvalue of $\mathbf{F}_i$ minimizes Eq. 4. However, since the interpolation between dyadic tensors is separately performed on each pair of eigenvectors the matrix $\mathbf{M} = [\mathbf{m}_i]$ is not generally orthogonal. The orthogonal matrix closest to $\mathbf{M}$ can be obtained by minimizing:

$$w_1\|\mathbf{x}_1 - \mathbf{m}_1\|^2 + w_2\|\mathbf{x}_2 - \mathbf{m}_2\|^2 + w_3\|\mathbf{x}_3 - \mathbf{m}_3\|^2 \ , \tag{6}$$

where $[\mathbf{x}_i]$ is an orthogonal matrix, and w_i are the eigenvalues computed by the LI method [5], which assigns different weights to each eigenvector term according to the interpolated tensor shape. Equation 6 can be rewritten in a matrix form:

$$\begin{aligned} \|(\mathbf{M} - \mathbf{X})\mathbf{W}\|_F^2 &= \mathrm{tr}\left\{(\mathbf{M}\mathbf{W} - \mathbf{X}\mathbf{W})(\mathbf{M}\mathbf{W} - \mathbf{X}\mathbf{W})^T\right\} \\ &= \mathrm{tr}\left\{(\mathbf{M}\mathbf{W})(\mathbf{M}\mathbf{W})^T\right\} + \mathrm{tr}\left(\mathbf{X}\mathbf{W}\mathbf{W}^T\mathbf{X}^T\right) - 2\mathrm{tr}\left(\mathbf{M}\mathbf{W}^2\mathbf{X}^T\right) \\ &= \|\mathbf{M}\mathbf{W}\|_F^2 + \|\mathbf{W}\|_F^2 - 2\mathrm{tr}\left(\mathbf{M}\mathbf{W}^2\mathbf{X}^T\right) \ , \end{aligned} \tag{7}$$

where $\mathbf{X} \in \mathrm{O}(3)$ and $\mathbf{W}^2 = \mathrm{diag}(w_i)$. Minimizing Eq. 7 is achieved by maximizing:

$$\mathrm{tr}\left(\mathbf{M}\mathbf{W}^2\mathbf{X}^T\right) = \mathrm{tr}\left(\mathbf{U}\mathbf{\Sigma}\mathbf{V}^T\mathbf{X}^T\right) = \mathrm{tr}\left(\mathbf{V}^T\mathbf{X}^T\mathbf{U}\mathbf{\Sigma}\right) \leq \mathrm{tr}\left(\mathbf{\Sigma}\right) \ , \tag{8}$$

where $\mathbf{U}$, $\mathbf{\Sigma}$ and $\mathbf{V}$ are obtained from the singular value decomposition (SVD) of $\mathbf{M}\mathbf{W}^2 = \mathbf{U}\mathbf{\Sigma}\mathbf{V}^T$, implying that Eq. 8 is maximized when $\mathbf{V}^T\mathbf{X}^T\mathbf{U} = \mathbf{I} \Leftrightarrow \mathbf{X} = \mathbf{U}\mathbf{V}^T$. Therefore, the interpolated tensor orientation $\mathbf{R_C} = [\mathbf{e_{C}}_i]$ can be obtained by replacing the singular values with ones from the SVD of $\mathbf{M}\mathbf{W}^2$. If the determinant of $\mathbf{R_C}$ is -1, then $\mathbf{R_C}$ should be negated to be a right-handed rotation matrix.

3 Methods

Synthetic Tensors. Using the EU, LE, GL, quaternion-based (QT) and dyadic tensor-based (DY) methods, interpolation was performed between two tensors of the same shape ($J_i = \{1, 0.5, 0.8\}$), and different orientations whose angles between each pair of eigenvectors are 82°, 45° and 64°. LI was used for tensor shape interpolation and combined with QT and DY for complete tensor interpolation.

Real DT-MRI Data. The rabbit heart DT-MRI data was acquired using a 7T Bruker Biospin scanner, and a 3D fast spin echo sequence with the following imaging parameters: TE/TR = 30/500 ms, b-value = 1000 s/mm^2, 24 diffusion gradient encoding directions, 6 nulls, and RARE factor two. The in-plane imaging resolution was 0.5×0.5×0.80 mm obtained by using a 96×96 encoding matrix, 72–96 slices and a 48×48×54–72 mm imaging volume. The pig heart DT-MRI data was acquired using a Siemens 1.5T Avanto and a 3T Trio scanner, and a 2D readout-segmented echo-planar pulse sequence with the following imaging parameters: TE/TR = 80/6800 ms, b-value = 1000 s/mm^2, 30 diffusion gradient encoding directions, one null, 15 readout segments, and 8-10 averages. The in-plane imaging resolution was 1×1×3 mm obtained by using an 150×150 encoding matrix, 43–44 slices and a 150×150×129–132 mm imaging volume. Diffusion tensors were estimated without zero padding and with linear regression.

Evaluation Procedure. The same tensor orientation evaluation procedure proposed in [5] was applied to the two rabbit and two pig heart DT-MRI datasets. The median autocorrelation (AC) length for every dimension was computed in each tensor invariant (J_i) map of the segmented myocardium. The myocardial DT-MRI volume was down-sampled in each dimension by a factor of the smallest integer not less than the median AC length for each tensor invariant map, and trilinear tensor orientation interpolation was performed with the EU, AI, LE, GL, QT and DY methods at the removed voxels using the remaining data. Then the interpolated tensor orientations by each method were compared to the originally measured data by computing the angle difference between each pair of eigenvectors. Subsequently the population of the angle difference data

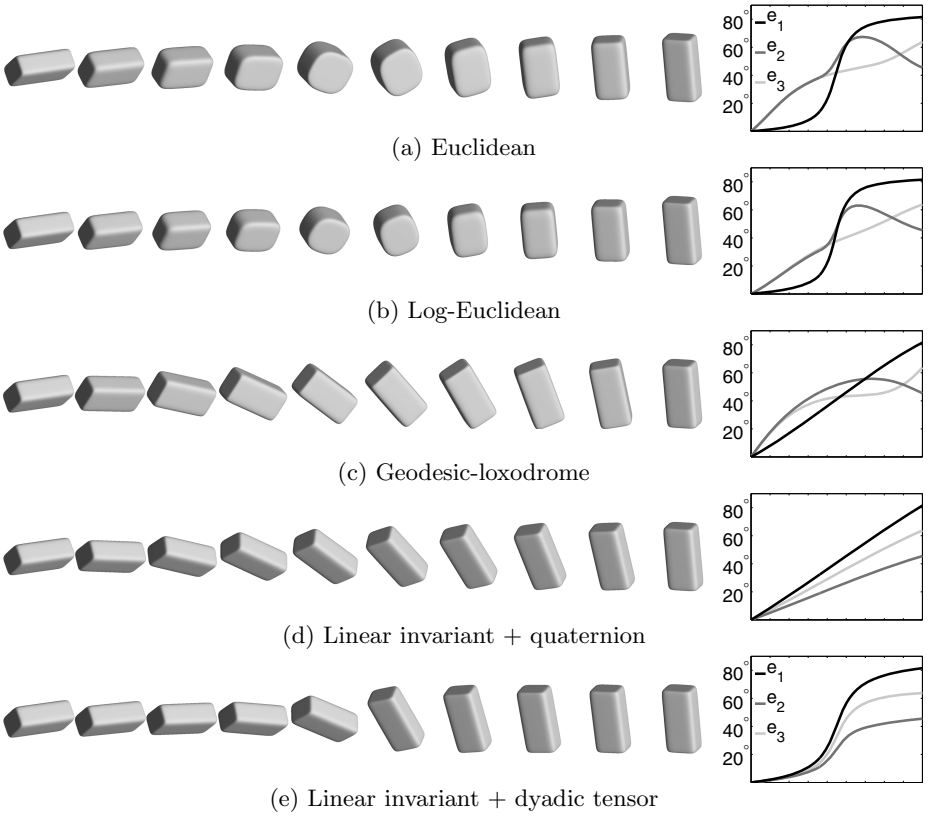

(a) Euclidean

(b) Log-Euclidean

(c) Geodesic-loxodrome

(d) Linear invariant + quaternion

(e) Linear invariant + dyadic tensor

Fig. 1. Interpolation between two synthetic tensors of equal shape and different orientation. The angle between every pair of the primary, secondary and tertiary eigenvectors is monotonically interpolated only in (d) and (e). All the tensor-based methods (a), (b), and (c) fail to monotonically interpolate the angle between the secondary eigenvectors.

was spatially decorrelated by decimating the data in every dimension by the smallest integer not less than the AC lengths, and the decorrelated data was bootstrapped 1000 times by random sampling with replacement to compute the 95% confidence interval (CI) about the median.

4 Results

Synthetic Example. Figure 1 shows an example of interpolation between two synthetic tensors with the same shape and different orientations using the EU, LE, GL, LI+QT and LI+DY methods. Tensors are visualized as superquadric glyphs [13], and plots of each eigenvector's angle relative to the leftmost tensor's orientation are shown along the interpolation paths. EU and LE fail to preserve the tensor shape during rotation, but GL, LI+QT and LI+DY maintain the

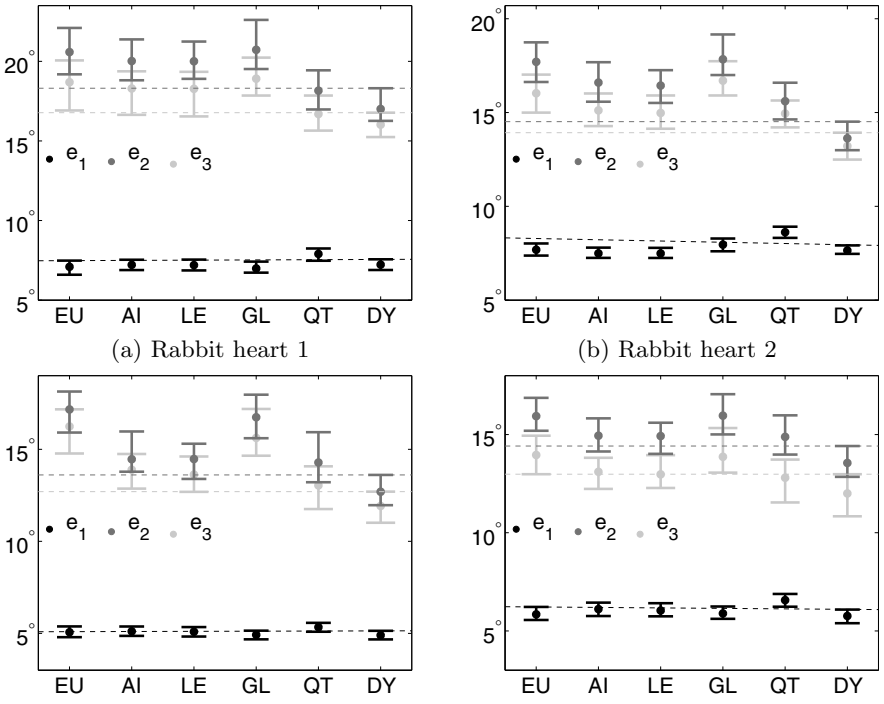

(a) Rabbit heart 1 (b) Rabbit heart 2

(c) Pig heart 1 (d) Pig heart 2

Fig. 2. Bootstrap statistics for eigenvector orientation errors (angle differences) relative to real DT-MRI data. Each dot represents the median angle difference, and each error bar represents the bootstrapped 95% CI of the median. The (black, dark gray, and light gray) dashed lines represent the upper limits of DY's CIs associated with the (primary, secondary, and tertiary) eigenvectors, which define whether or not DY's CIs overlap with the others'. DY introduces the least error to the secondary and tertiary eigenvector orientations, and similar errors to the primary eigenvector orientation compared to the tensor-based methods (EU, AI, LE and GL).

tensor shape. With respect to tensor orientation, QT and DY monotonically interpolates the angle of every eigenvector. The tensor-based methods (EU, LE and GL), however, fail to monotonically interpolate the angle of the secondary eigenvector.

DY's monotonic interpolation of each eigenvector needs to be more carefully investigated. Each method has a distinct interpolation path between tensor orientations, and QT's path is explicitly the minimum rotation path. Monotonic interpolation of eigenvectors and/or the minimum rotation path does not imply interpolation of tensor orientation with the least error. Therefore, we experimentally evaluated each method using real DT-MRI data.

Evaluation Statistics. The smallest integers not less than the median AC lengths were 2, 2, and 3 for the rabbit heart data and 3, 3, and 2 for the pig heart

data in the x–, y– and z–directions, respectively. Figure 2 shows the bootstrap statistics of angle differences between each eigenvector pair from the original and interpolated tensor orientations.

Comparison of the orientation errors between methods reveals that each method performs consistently across the various data sets (e.g. errors for recovering $\mathbf{e}_1$ significantly decrease from QT to DY). QT's $\mathbf{e}_1$ median error, however, is significantly higher than all other methods (i.e. 95% CI does not overlap) for the rabbit data, but not for the pig data. DY performs similarly to conventional tensor interpolation methods for recovering $\mathbf{e}_1$ in both rabbit and pig DT-MRI data.

DY has the lowest median error for recovery of both $\mathbf{e}_2$ and $\mathbf{e}_3$ compared to all other methods. Notably, DY has a significantly lower median recovery error for $\mathbf{e}_2$ and $\mathbf{e}_3$ compared to either EU or GL for all four datasets.

5 Conclusion

Accurate interpolation of myofiber and myolaminar sheet orientations is essential for computational modeling of cardiac mechanics and electrophysiology (EP). Cardiac mechanics and EP modeling requires accurate tensor orientation information at every computational node in order to assign correctly the axes of anisotropic electrical activation.

The comparison results show that DY performs significantly better than the tensor based methods, especially EU and GL, for recovery of each component of cardiac microstructural orientation. In particular, the improvement in recovery of the secondary and tertiary eigenvectors is important for recovery of myolaminar sheet orientation. Note that QT's minimum rotation path has significantly larger median errors for recovery of the primary eigenvector than DY's interpolation path.

LI+DY is a commutative, computationally efficient (compared to GL's numerical solution), and mathematically unambiguous tensor interpolation method that most accurately interpolates both cardiac microstructural shape [5] and orientation. Further investigations using brain DT-MRI data and the same evaluation process may be needed to evaluate if the most accurate interpolation is dependent on the underlying tissue characteristics. Furthermore, the required tensor interpolation accuracy for cardiac mechanics and EP simulations remains incompletely understood.

References

1. Basser, P.J., Mattiello, J., LeBihan, D.: Estimation of the effective self-diffusion tensor from the NMR spin echo. J. Magn. Reson. B 103(3), 247–254 (1994)
2. Ennis, D.B., Kindlmann, G.: Orthogonal tensor invariants and the analysis of diffusion tensor magnetic resonance images. Magn. Reson. Med. 55, 136–146 (2006)
3. Kindlmann, G., Ennis, D.B., Whitaker, R.T., Westin, C.F.: Diffusion tensor analysis with invariant gradients and rotation tangents. IEEE Trans. Med. Imaging 26(11), 1483–1499 (2007)

4. Kindlmann, G., San José Estépar, R., Niethammer, M., Haker, S., Westin, C.-F.: Geodesic-loxodromes for diffusion tensor interpolation and difference measurement. In: Ayache, N., Ourselin, S., Maeder, A. (eds.) MICCAI 2007, Part I. LNCS, vol. 4791, pp. 1–9. Springer, Heidelberg (2007)
5. Gahm, J.K., Wisniewski, N., Kindlmann, G., Kung, G.L., Klug, W.S., Garfinkel, A., Ennis, D.B.: Linear invariant tensor interpolation applied to cardiac diffusion tensor MRI. In: Ayache, N., Delingette, H., Golland, P., Mori, K. (eds.) MICCAI 2012, Part II. LNCS, vol. 7511, pp. 494–501. Springer, Heidelberg (2012)
6. Kung, G.L., Nguyen, T.C., Itoh, A., Skare, S., Ingels Jr., N.B., Miller, D.C., Ennis, D.B.: The presence of two local myocardial sheet populations confirmed by diffusion tensor MRI and histological validation. J. Mag. Res. Imaging 34(5), 1080–1091 (2011)
7. Tseng, W.Y., Reese, T.G., Weisskoff, R.M., Wedeen, V.J.: Cardiac diffusion tensor MRI in vivo without strain correction. Magn. Reson. Med. 42(2), 393–403 (1999)
8. Pennec, X., Fillard, P., Ayache, N.: A Riemannian framework for tensor computing. Int. J. Comp. Vis. 66, 41–66 (2006)
9. Arsigny, V., Fillard, P., Pennec, X., Ayache, N.: Log-Euclidean metrics for fast and simple calculus on diffusion tensors. Magn. Reson. Med. 56, 411–421 (2006)
10. Yang, F., Zhu, Y.M., Magnin, I.E., Luo, J.H., Croisille, P., Kingsley, P.B.: Feature-based interpolation of diffusion tensor fields and application to human cardiac DT-MRI. Med. Image Anal. 16(2), 459–481 (2012)
11. Blow, J.: Understanding slerp, then not using it. The Inner Product (April 2004)
12. Basser, P.J., Pajevic, S.: Statistical artifacts in diffusion tensor MRI (DT-MRI) caused by background noise. Magn. Reson. Med. 44, 41–50 (2000)
13. Ennis, D.B., Kindlmann, G., Rodriguez, I., Helm, P.A., McVeigh, E.R.: Visualization of tensor fields using superquadric glyphs. Magn. Reson. Med. 53, 169–176 (2005)